

## **Seismic monitoring of steamfloods in heavy oil reservoirs: A review**

John J. Zhang and Laurence R. Bentley

A colour version of this paper is available on the CREWES 2001 Research Report CD.

### **ABSTRACT**

Steamfloods are used to improve heavy oil recovery. There are a variety of methods that can be used to detect thermal fronts and fluid movements. These methods include surface seismic, cross-well seismic tomography, cross-well electromagnetic tomography and passive seismic monitoring. The most commonly used seismic attributes are velocity, time delay, and reflection amplitude. AVO analysis and statistical methods such as discriminant analysis are improving the resolution and accuracy of seismic monitoring. Case studies from Indonesia and North America demonstrate the resolution of seismic monitoring and the relationship to reservoir changes due to steam injection.

### **INTRODUCTION**

The fundamental principle governing fluid movement through porous media is Darcy's law, in which fluid flux is proportional to the hydraulic head gradient and permeability but varies inversely with fluid viscosity. A major task of reservoir engineers is to improve these conditions for hydrocarbon recovery. Thermal methods, particularly steamflood, have been successfully used to improve heavy oil recovery. In most cases, increased oil recovery is due to a tremendous reduction of the heavy oil's viscosity at high temperature (Figure 1).

World reserves of heavy oil have been estimated to be greater than 4 trillion bbl (Thakur et al., 1998). The total bitumen reserves recoverable by thermal methods in Alberta, Canada and in Venezuela exceed 600 billion bbl with a production potential of 2 million bbl per day (Thakur et al., 1998). Canada's future increase in petroleum production will depend on heavy oil production. Nur (1989) estimates that heavy oil reserves can supply the world's fuel needs for 200-1000 years. Thus, it is important for geoscientists and engineers to develop efficient production technologies.

Efficient thermal recovery depends on the knowledge of the location of thermal fronts and fluid movements in reservoirs. A poor understanding of steam-flow directions, rates and sweep efficiency can lead to poor injection-well placement, inefficient intervals of perforation and inappropriate surface steam facility planning (Lumley et al., 1995). Due to very low bulk modulus of unconsolidated sands, the bulk modulus and compressional velocities of oil-saturated sands are very sensitive to the bulk modulus of oil according to the principles of rock physics (Zhang, 2001). When high-temperature steam is injected into heavy oil reservoirs, the bulk modulus of heavy oil undergoes a considerable decrease, causing a large decrease in the bulk modulus and compressional velocity of heavy oil sands. The fluid pressure increase

due to steam injection causes a reduction in the effective stress and the dry bulk modulus of the sand, further decreasing the elastic moduli and velocities of heavy oil sands. This prediction is well supported by experimental results, in which the compressional velocity of heavy-hydrocarbon-saturated sandstones and sands decrease markedly with increasing temperature (Tosaya and Nur, 1984; Wang and Nur, 1988). Wang and Nur (1988) give a rough estimate of compressional velocity changes of 10-15% per  $100^{\circ}\text{C}$  decrease for well-consolidated heavy oil sandstones and 15-40% per  $100^{\circ}\text{C}$  decrease for unconsolidated heavy oil and tar sands (see Figure 2). In addition, the quality factor,  $Q$ , may also change because the number of cracks changes, and the frequency, at which absorption peaks, will change due to the large change in fluid viscosity. These theoretical and laboratory results provide a rock physics basis for time-lapse seismic surveys to monitor steam floods.

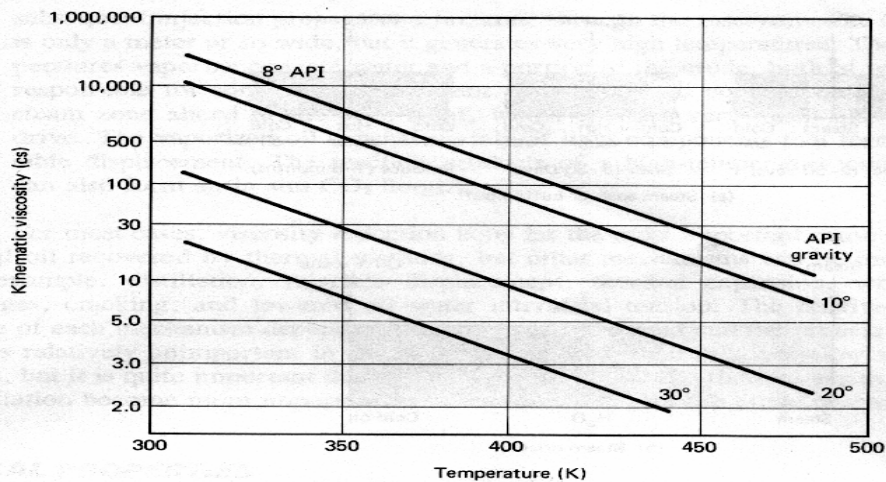


FIG. 1. Effect of temperature on crude oil viscosity (Lake, 1989)

In this paper, we focus on steam injection. First, the distribution of fluids, temperature, and pressure, and the velocity changes in different zones around the steam front, are briefly discussed. A number of seismic techniques to trace steam floods are summarized. Finally, successful cases in Indonesia and North America are analysed with an emphasis on the steam project in Duri field.

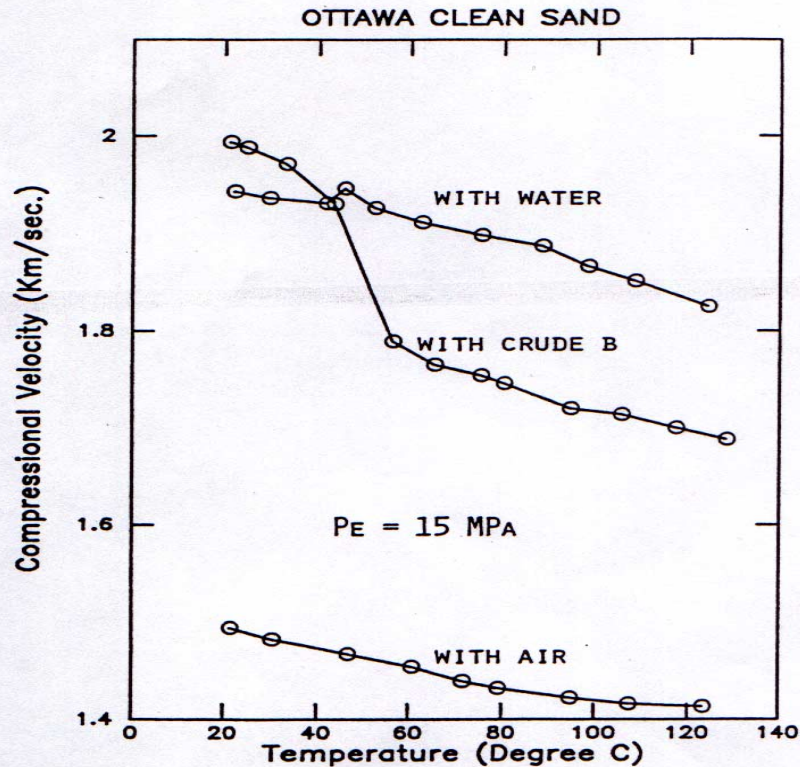


FIG. 2.  $V_p$  in the Ottawa clean sand saturated with crude B versus temperature (Wang and Nur, 1988).

### STEAM FLOOD DISTRIBUTION MODEL

When steam is introduced, the zone immediately next to the well has the highest pressure and temperature, and new cracks can be generated due to differential thermal expansion of minerals and effective stress relief. Steam drives nearly all the heavy oil and connate water out of the pore space. This process is equivalent to complete steam substitution. The much lower bulk modulus of steam, reduction in effective stress and generation of cracks contribute to a large decrease in compressional velocity. In seismic sections, there would be a higher amplitude reflection on the reservoir bottom and top (bright spots), and a time delay on the reservoir bottom reflection. The density in the zone decreases.

Due to heat transfer to the surrounding rocks and fluids, the steam front will cool down and condense into hot water that constitutes the second zone next to the steam zone. It can be regarded as hot water substitution. Depending on temperature and pressure, cracking may occur. Whether the compressional velocity increases or decreases is largely determined by the initial fluid state before steam injection. For example, in Duri field, Indonesia, heavy oil contained gas due to pressure reduction from primary recovery before steam injection. After steam injection, compressional velocity increased due to a homogeneous mixture of heavy oil and gas being replaced by hot water.

Further away from the injection well is the hot water drive zone, where hot water is mixed with hot oil. Similarly, compressional velocity may increase or decrease, depending on the initial state before steam injection.

The fourth zone is heated by thermal conduction, but the oil has not been displaced by hot water. Temperature and pressure are less than the other three zones. Compressional velocity may decrease depending on the initial state before steam injection. This zone is most suitable for oil production.

Outside of the heated zones is the cold oil bank. Although the temperature does not increase, the fluid pressure rises due to pressure propagation. The pressure change has no appreciable effect on the bulk modulus of heavy oil except when free gas is redissolved due to the pressure increase.

The five zones are summarized in Figure 3.

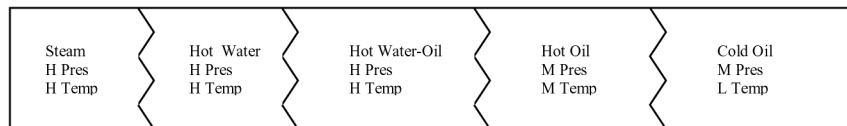


FIG. 3. An idealized model of steamflood fluid flow (after Lumley, 1995)

## SEISMIC METHODS FOR STEAMFLOOD MONITORING

As stated above, the compressional velocity in the steam zone immediately around the injector well decreases substantially and the density decreases with the substitution of steam for heavy oil. The hot water and hot water drive zones may undergo a decrease or increase, depending on the initial conditions before steam injection. The changes in velocity and density make it possible to monitoring thermal fronts by repeat seismic surveys. There are a number of seismic methods available to achieve this goal, including surface seismic and cross-well seismic.

Early work on seismic monitoring of steam-based EOR started in the 1980s. Britton et al. (1983) demonstrated that velocity anomalies occurred at steam injection sites at the Street Ranch pilot project in Texas. Pullin et al. (1987) used time-lapse seismic surveys to investigate the response in the Athabasca heavy-oil reservoir sands. Greaves and Fulp (1987) used time-lapse 3-D seismic data to monitor the propagation of a fire-flood in Texas. Laine (1987) used time-lapse seismic tomography to observe changes at a heavy-oil steam flood. Tomography was also used by Paulsson et al. (1992), Paulsson et al. (1994), Macrides et al. (1988) and Bregman et al. (1989) to monitor the reduction in velocity caused by steamfloods and a fire-flood in heavy-oil reservoirs.

**Surface seismic:** 3-D seismic monitoring surveys are commonly employed with an initial baseline survey for the undisturbed reservoir. Any amplitude change or time delay or frequency change in the reservoir zone in repeat seismic surveys can be attributed to changes in the reservoir due to steam floods. Amplitudes of the extracted horizons above or below the reservoir can be used to map the relative changes

between the initial survey and repeat surveys. The anomalies are interpreted in terms of changing reservoir conditions due to steam injection. The occurrence of bright spots or dim spots on the reservoir top and bottom in repeat seismic surveys may indicate the steam-swept zones. Figure 4 is a geological model of a reservoir section (den Boer and Matthews, 1988). Figure 5 is the pre-injection synthetic seismic response calculated based on Figure 4 (den Boer and Matthews, 1988). Figure 6 is the post-injection seismic response (den Boer and Matthews, 1988).

A comparison of Figure 5 with Figure 6 reveals the marked increase at the injector location in the amplitude of the reflections corresponding to the top and bottom of the tar sand (den Boer and Matthews, 1988) and the increased reflection times below the reservoir. Isochron maps can be constructed by picking reflections above and below the heated zone and computing the time difference. The time delay is calculated by subtracting the isochron for the pre-injection response from the one for the post-injection response. The areal extent can be inferred from the size of the time delay anomaly. Figure 7 is the map of the time delay computed from data in the Gregoire Lake oil field, northern Alberta. It demonstrates an excellent correlation between the position of injection wells and the position of the time delay anomalies (den Boer and Matthews, 1988). Another seismic attribute is the change in frequency. In Figure 8, the time window above the reservoir shows the same pattern of frequency distribution for pre-injection and post-injection. The time window below the reservoir, however, is markedly different in frequency distribution with more high frequencies attenuated in post-injection. High-frequency energy surfaces can be contoured so that the low frequency values correspond to high-frequency attenuation (Eastwood, 1994).

The previous techniques are incapable of resolving the vertical distribution of thermal movement. They can be augmented by inverting seismic data for velocity distribution. Subtracting velocity in post-injection from that in pre-injection yields velocity difference, which can be sliced horizontally or vertically to reveal thermal fronts (den Boer and Matthews, 1988). Figure 9 is a cross-section vertically sliced from the velocity difference volume with the anomalies consistent with two injection wells. It gives a detailed representation of the vertical distribution of steam floods.

**Cross-well seismic:** Time-lapse cross-well seismic tomography has been successfully applied to steam injection imaging and may provide a viable tool for reservoir monitoring. Mathisen et al. (1995) recorded twenty-seven cross-well seismic surveys across a California heavy oil field during a three and half month period (before, during and after a steam injection cycle) with a cemented-receiver cable. Based on these data, they established by tomography  $V_p$  and  $V_s$  cross-well distribution models at different times. Figure 10 shows the  $V_p$  difference contours at day 5, day 46 and day 109 after steam injection. The strong velocity decrease anomalies are controlled by the injection wells. The configuration and size of the low-velocity zones represent the manner in which the steam flood moved within the reservoir.

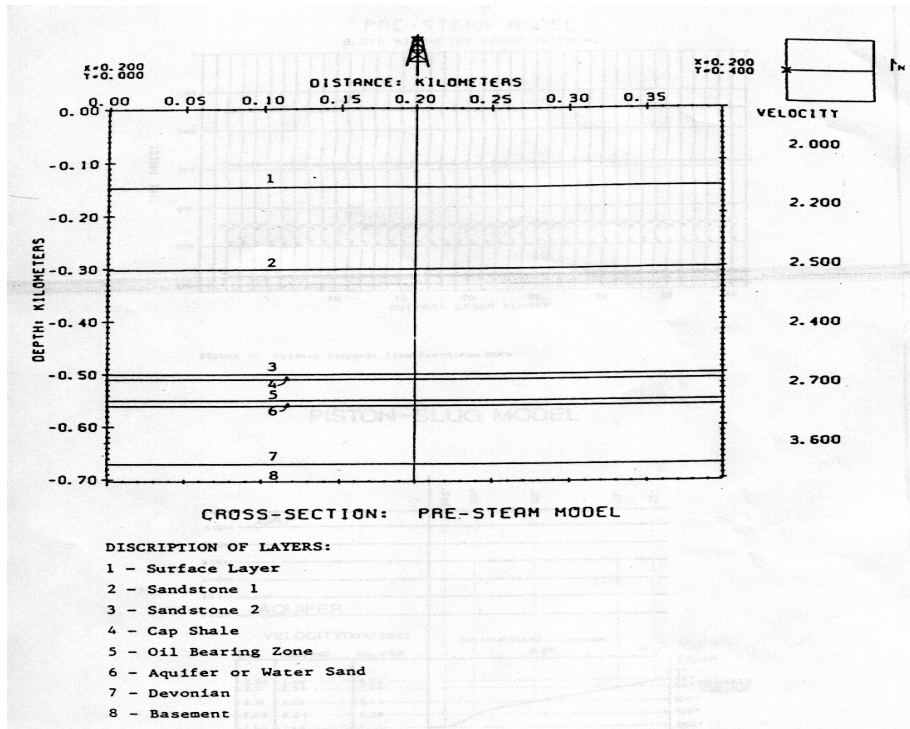


FIG. 4. Geological cross-section (den Boer and Matthews, 1988)

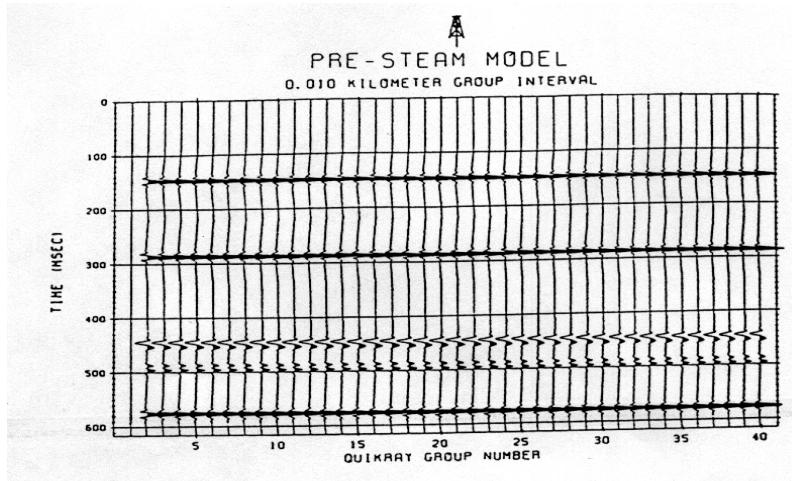


FIG. 5. Seismic response from pre-steam model (den Boer and Matthews, 1988)

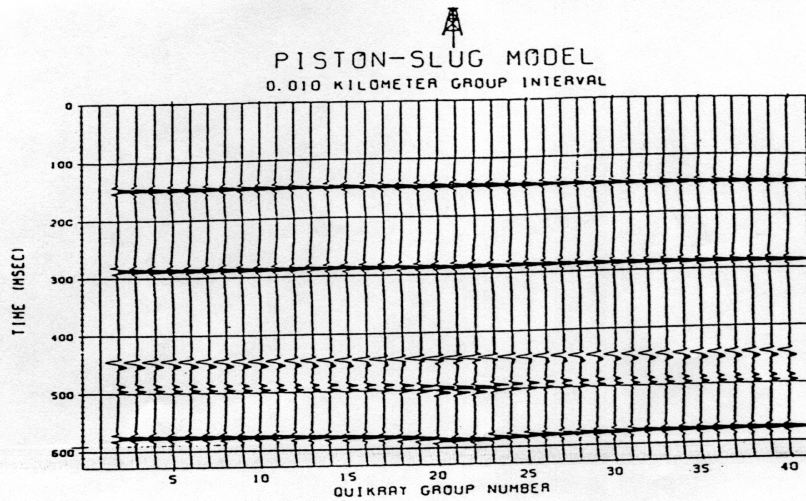


FIG. 6. Seismic response from Piston-Slug model (den Boer and Matthews, 1988)

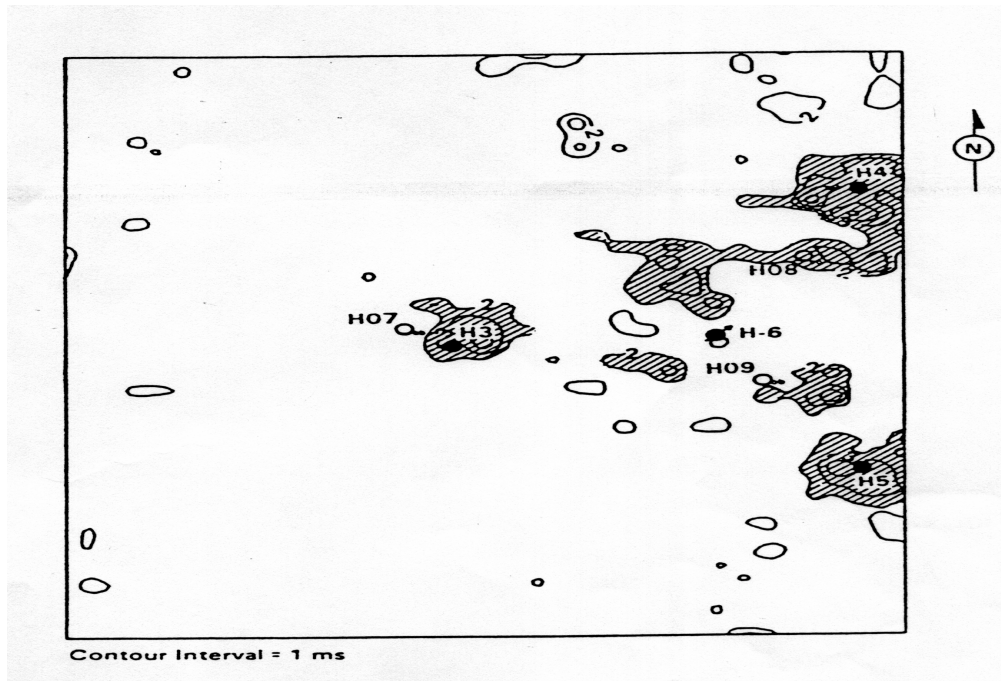


FIG. 7. Pushdown map illustrating areal distribution of the heated tar sands (den Boer and Matthews, 1988)

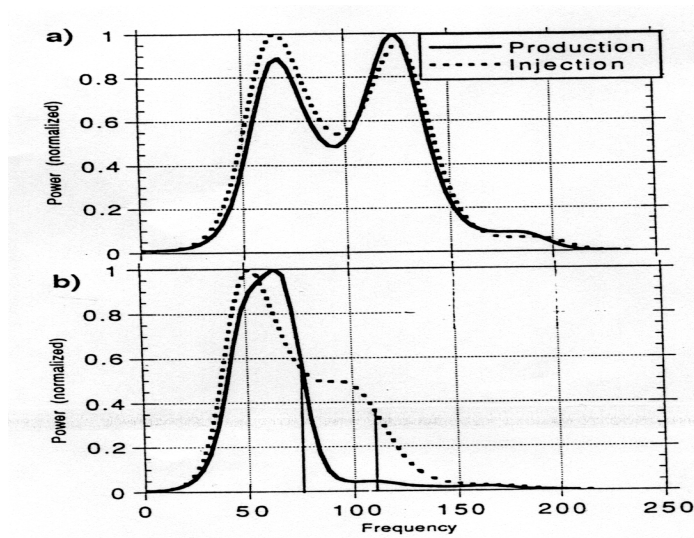


FIG. 8. (a) The spectra above the reservoir are almost identical in frequency content. The spectra below the reservoir (b) are markedly different, especially for the higher frequency. In both cases, the data have been normalized to the amplitude at peak frequency (Eastwood and Blakeslee, 1994).

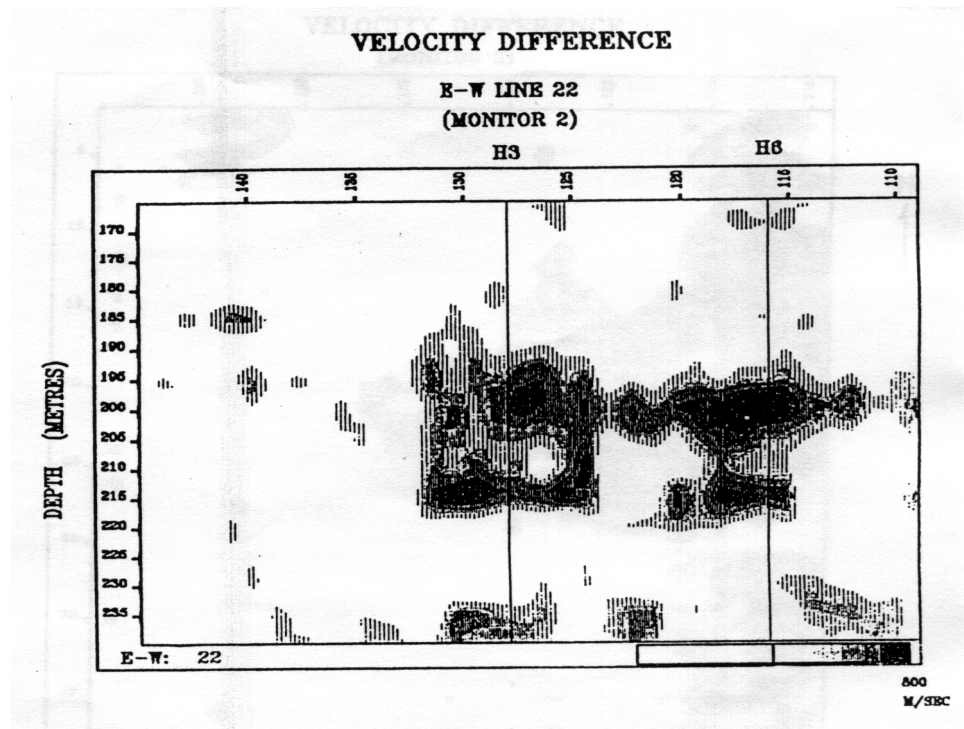


FIG. 9. Velocity slice through velocity difference cube for Monitor survey #2 (den Boer and Matthews, 1988).

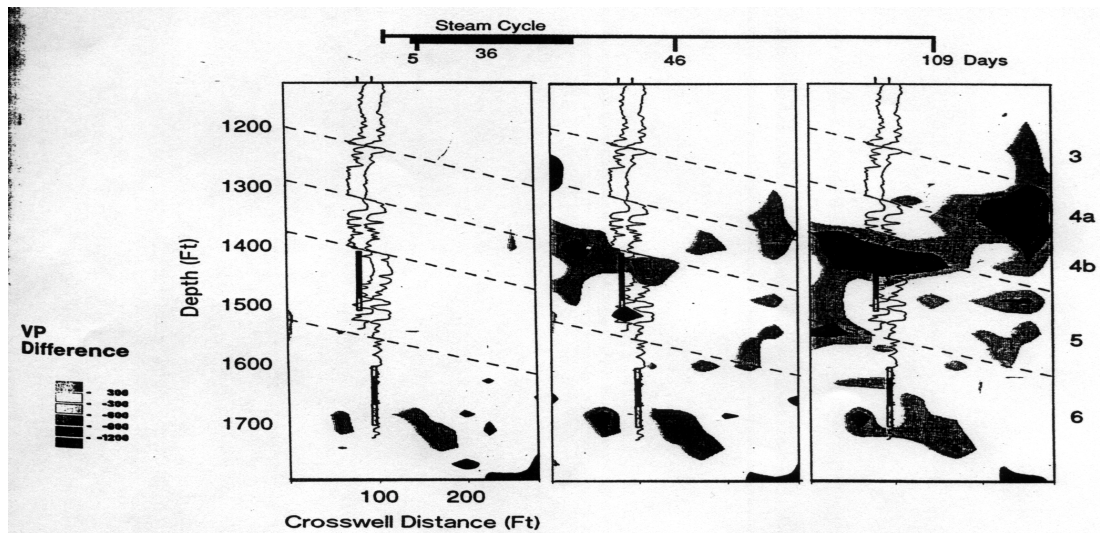


FIG. 10. P-wave difference tomograms illustrating location and amount of velocity decrease as a result of steam injection. After 46 days, the largest decrease occurs near the cyclic steam injectors. After 119 days, a large velocity decrease occurs in zone 4 as a result of continuous down-dip steaming (Mathisen et al., 1995).

**Cross-well EM:** Cross-well electromagnetic data can provide complementary information to seismic data. Seismic data reveal the velocity and acoustic impedance distribution. The fluid distribution is related to velocity and acoustic impedance in a complicated way. Seismic methods are sometimes not sensitive to fluids. On the other hand, EM measurements are often sensitive to pore fluids. Wilt et al. (1997) conducted a series of cross-well EM surveys before steam injection and after at Lost Hills of central California. High-resistivity zones correspond to oil sands while low-resistivity parts represent steam injection and water zones. The steam movement within the reservoir was clearly imaged by resistivity distribution.

**Passive seismic:** In steam injection, new cracks can be generated due to differential thermal expansion and effective stress relief at high pressure and temperature. Collapse of steam bubbles in the presence of certain oils marks a significantly greater rate of heat transfer than normal condensation (Gendzwill, 1992). The phase change and cracking are a source of seismic energy. If microseismic events from these sources after steam injection are detected and recorded on enough geophones, they can be located in 3D space by using a method of triangulation (Snell et al., 1999; see Figure 11). Consequently steam-fronts can be tracked and delineated within the reservoir. Gendzwill (1992) planted 16 geophones in 14m-deep holes over an area of 3 hectares for steam flood monitoring. Unfortunately microseismic activity due to cracking was not detected after steam injection. The possible reason is that cohesionless heavy-oil sands failed at low effective stress, giving off very small seismic emission (Agar et al., 1986, 1987; Gendzwill, 1992). Seven seismic events that appeared to be caused by phase-change during steam injection were detected. As

shown in Figure 12, the events numbered in chronological order can roughly measure the movement of steam flood.

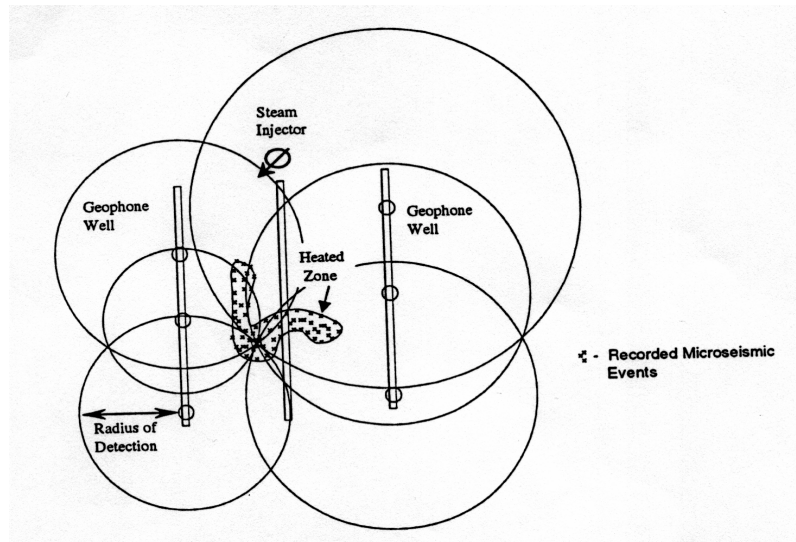


FIG. 11. Diagram of Event Location Using Triangulation. As microseismic events occur near a steam injector, geophones in offset wells record the events. If two or more geophones detect an event, the event can be located by triangulation (Snell et al., 1999).

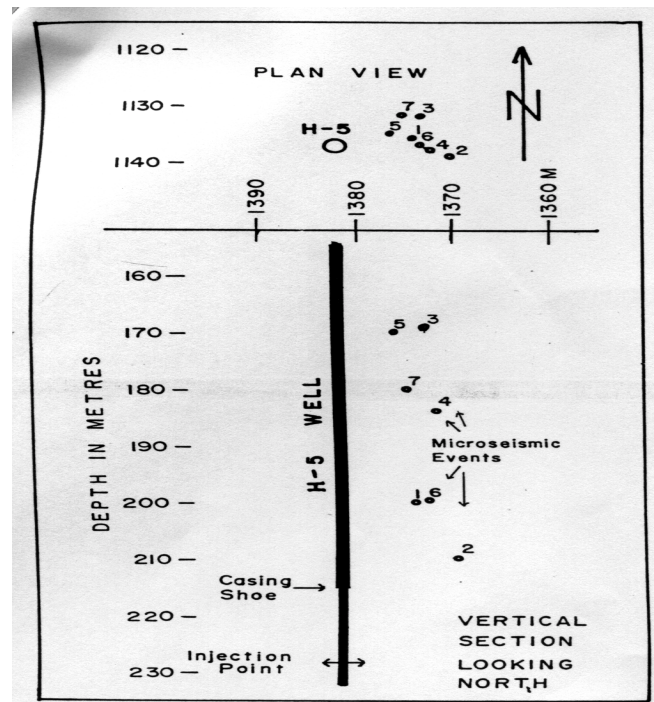


FIG. 12. Location map of deep events from well H-5. Events are numbered in chronological order. In plan view, all events are within one error unit of their mean position. The mean position is more than one error unit from the well axis. In vertical position, the events are separated by more than one error unit. The well diameter is not drawn to scale (Gendzwill, 1992).

## CASE REVIEW

There are a number of successful examples of seismic monitoring of steam injection around the world. The major characteristics for these reservoirs are unconsolidated sandstones or sands saturated with high-viscosity heavy oil buried at shallow depth. As a result, the compressional velocity and acoustic impedance are sensitive to the bulk modulus of pore fluids, which would undergo a considerable change during steam flood. In what follows, we give a brief review of the cases encountered in Indonesia and North America.

### Time-lapse monitoring of the Duri steamflood

Duri field is located on the island of Sumatra, Indonesia (Jenkins et al., 1997). The pilot study area has three early Miocene deltaic sandstone reservoirs: Upper Pertama, Lower Pertama and Kedua (Figure 13). These shallow reservoirs (350-750 ft) have excellent porosity of 30-38% and permeability (>1500 md). Sandstones are saturated with 30-60% heavy oil with API gravity of 22 and viscosities of 100-1000cp (Lumley, 1995). Initial pore pressure is 100 psi and ambient reservoir temperature is 100° F. Primary production only extracted a small portion of the original oil in place (5.4 billion bbl) due to high viscosity. The steamflood project began in 1985 and is currently the largest steamflood in the world. More than 900 injector wells inject approximately 1.25 million B/D steam into the reservoirs. The field currently produces 300,000 BOPD from more than 2700 producing wells. However, the heterogeneity of sandstone reservoirs can cause steam flood problems. Substantial volumes of oil can be left in unswept pockets and steam ‘cycling’ between the injector and the producer along high-permeability zones can waste considerable amounts of energy. If time-lapse seismic surveys can image steam fronts and fluid movements, these and other problems may be solved.

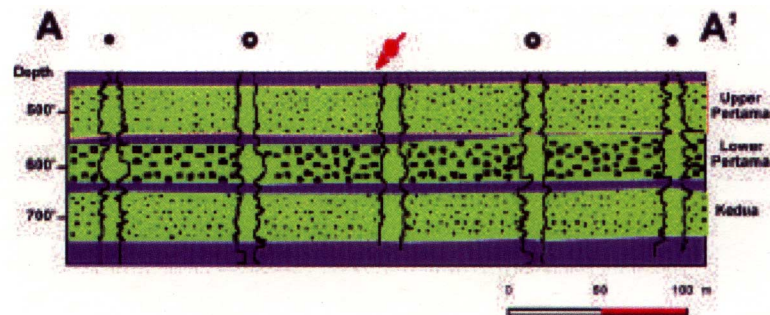


FIG. 13. Wireline log cross-section through the pilot area, showing the injection well, observation wells, and producing wells (Jenkins et al., 1997).

Two baseline and six monitor 3-D seismic surveys were recorded over the same steam injection pattern between 1992 and 1995. Figure 14 shows vertical sections from the seven data volumes. The steam injection interval is between 135 and 220ms. After two months of injection, a large time structure on the reservoir bottom reflection developed below the injection well. This time structure increased with time and reached a maximum after 31 months. The growth of the time structure is illustrated in Figure 15 by comparing the reflection times from reservoir bottom reflections at different times. After two months of injection, the traveltimes were shortened relative to the baseline. This indicates a large increase in velocity due to the steam flood. In addition, a time-sag formed in the region around the injector well and grew with time. After 31 months of steam injection, the reflections around the injector were delayed 12ms from the baseline, indicating a large decrease in velocity. Figure 16 shows the spatial distribution of the time structure. The difference in interval traveltimes from the top to the bottom of the reservoir between the baseline and repeat surveys are shown in colour. Green indicates no travel time difference between the baseline and repeat surveys. Blue represents pull-ups in the repeat surveys and yellow and red represents push-downs. After two months, a pull-up was observed, and after five months, it was extended but with a push-down immediately around the injector. The push-down increases afterwards. After 31 months, it also developed at the corner of the study area, close to injectors located just outside the pilot pattern.

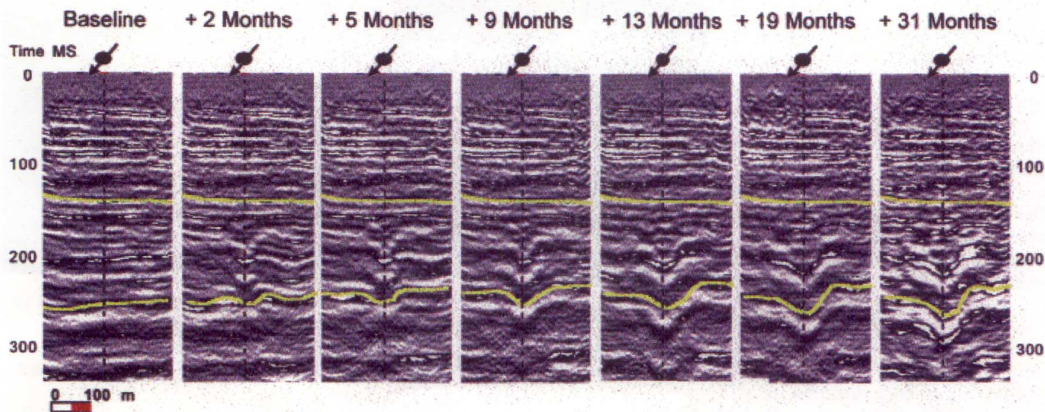


FIG. 14. Vertical seismic sections from baseline and monitor surveys. The yellow lines show the top and base of the steam injection interval. A synclinal shape develops within and below this interval after 2 months, and grows to about 20 ms after at 31 months. Note the data do not change above the steam zone (Jenkins et al., 1997).

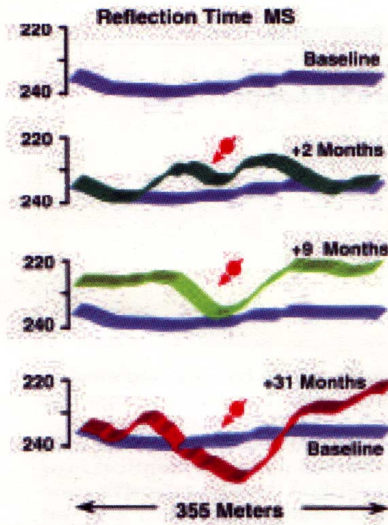


FIG. 15. Reflection times from the base of the steam interval for the baseline and monitors highlighting how pull-ups and push-downs develop (Jenkins et al., 1997).

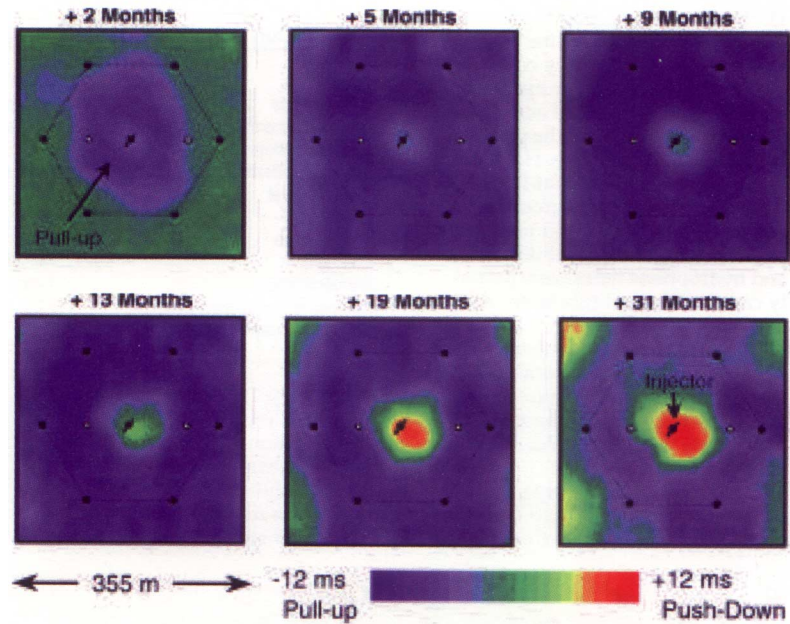


FIG. 16. Travel time difference between the baseline and monitor surveys. Green areas have the same interval traveltimes in both baseline and monitor surveys. Blue areas represent pull-ups in the monitor data with respect to the baseline. Yellow/red areas represent push-downs in the monitor data. A pull-up develops around the injector after 2 months and extends over the whole pattern after 5 months. Push-downs grow around the injector well to a maximum radius of 50m after 31 months of injection (Jenkins et al., 1997).

The velocity changes with time are consistent with reservoir simulation results (Figure 17). During primary production, the velocity drops from 7000 ft/s to 5500 ft/s (from point 1 to 2) due to the presence of ex-solved gas from heavy oil. The small amount of gas decreases the fluid bulk modulus substantially but has little effect on the bulk density. When steam is injected, high pore-pressure propagates from the injector to other parts of the field and gas re-dissolves in heavy oil. Consequently the velocity increases (from point 2 to 3). In the immediate vicinity of the injector, steam drives nearly all fluids. Steam has a bulk modulus close to the mixture of gas and heavy oil, but a much smaller density. So steam zones have a slightly higher velocity than the original state of the gas-heavy oil system. Thermal fronts then begin to heat heavy oil and the velocity declines (point 4). Steam zones expand outward from the injector and the velocity further decreases (point 5). The decrease around the injector is due to the buildup of pressure and temperature generated new cracks, which decrease the elastic moduli and velocities.

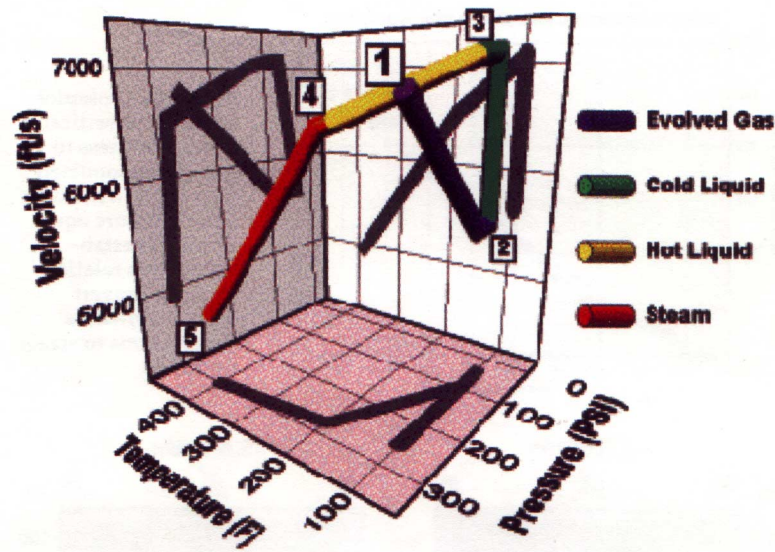


FIG. 17. Velocity changes for a single cell in the model as a function of pressure and temperature. Changes in pore fluid are indicated with colour. Velocity decreases during the primary production cycle before steam injection due to the presence of evolved hydrocarbon gas (point 1 to 2). At the beginning of steam injection the free gas is pushed back into solution and velocity increases (point 2 to 3). As injection continues, velocity decreases due to heat (point 3 to 4) and finally due to steam (point 4 to 5) (Jenkins et al., 1997).

### Seismic monitoring of thermal recovery in Cold Lake

The Cold Lake oilfield is located in Alberta, Canada. Heavy oil produces from the Clearwater formation in the Mannville group of lower Cretaceous. The reservoir is 420m below the surface (Sun, 2001) and consists of unconsolidated sandstones or sands with an average porosity of 32% and permeability of about 1 Darcy (Kalantzis, 1994). The reservoir has a net pay of 40m filled with bitumen, which has a very high viscosity of 150,000cp (Kalantzis, 1994). For heavy oil production, cyclic steam

stimulation (CSS) was first adopted to reduce viscosity. In CSS, steam is introduced into the reservoir through a well and then the well is returned to production after a brief shut-in period. Repeat CSS would reach the recovery limit of 25% due to a decline in OSR (Oil-Steam-Ratio) (Sun, 2001). The Follow-up Processes (FUPs) targeted the heated zones between the wells for infill drilling (After Sun, 2001). These heated zones were characterized by high temperature (due to CSS) and low pressure (due to production) and were expected to decrease in velocity and acoustic impedance chiefly due to the decrease in the bulk modulus of pore fluids. Despite the reduction of the bulk modulus of heavy oil, the reduction of the bulk modulus of the reservoir is mainly due to exsolution (methane and carbon dioxide) (Jack, 1998; Sun 2001).

Due to the unavailability of the baseline surveys, the seismic data in an area with no CSS wells were contrasted with those close to CSS wells to find the seismic attributes that were most sensitive to reservoir conditions (after Jack, 1998). The key seismic attributes are time delay (or sag), amplitude and frequency (Sun, 2001). Figure 18 is a map of the amplitude and spectral attributes that separate the heated zones from the unheated zones. There are also other seismic attributes derived from seismic data. These seismic attributes are correlated, and for optimal results, the principal components were extracted for discriminant analysis (Jack, 1998; Sun 2001). Figure 19 shows the result of discriminant analysis and the resulting steam distribution.

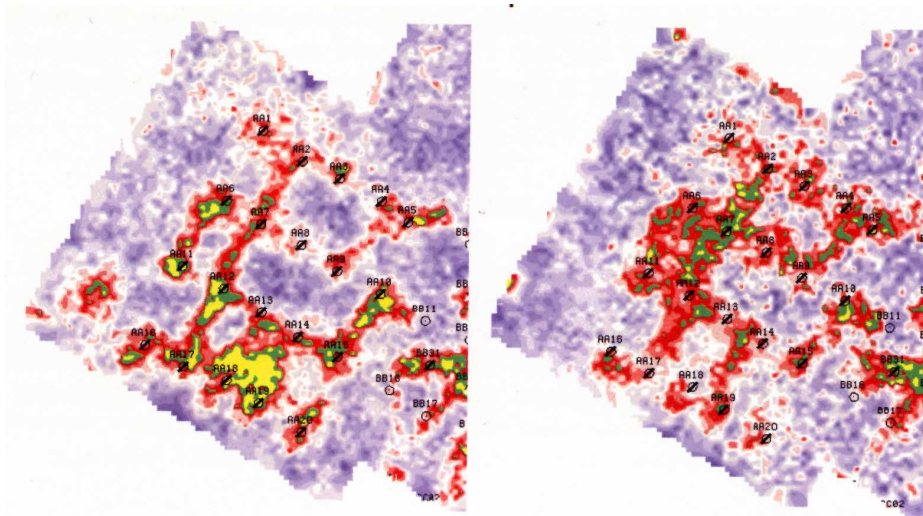


FIG. 18. Amplitude (left) and spectral attributes (right) showing heated zones (Jack, 1988).

Isaac (1996) used two 3-D seismic surveys and two time-lapse multicomponent (3-C) surveys to study Cold Lake. She found that amplitude anomalies were due to zones of low velocity in the vicinity of the steamed reservoir zones. The  $V_p/V_s$  ratio was lower during steaming than during production. Areas of heated and cold reservoir

mapped from  $V_p/V_s$  ratios agreed with the P-P 3-D surveys. AVO analysis confirmed that the amplitude anomalies were due to low velocity zones.

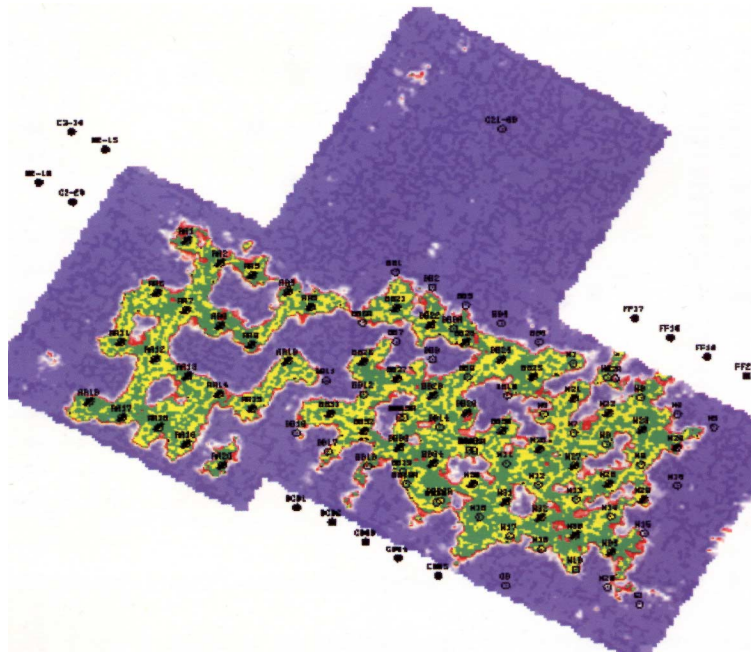


FIG. 19. Results of discriminant analysis showing heated zones (Jack, 1998)

### Crosswell seismic monitoring of a California heavy oil field

Cyclic steam has been injected to heat the reservoir for low-API (10 to 12) heavy oil production (Mathisen et al., 1995). To monitor thermal fronts between wells, twenty-seven crosswell seismic surveys were acquired during a three-and-half-month period (before, during and after a steam injection cycle) with a cemented-receiver (Mathisen et al., 1995). The baseline (before injection) S-wave (Figure 20) tomogram image shows the velocity distribution caused by the lithofacies-controlled porosity variations. The baseline P-wave image is similar but contains significant pore fluid effects. It is found that S-wave tomograms do not change with time. Time-lapse S-wave tomograms acquired during the steam cycle, shortly after cycle and after three and half months are very similar to the baseline S-wave tomogram (Mathisen et al., 1995). In contrast, P-wave tomograms change with time. Decreases in the velocity are associated with the injector location (Figure 10). In addition, Poisson's ratio tomograms also change with time. The post-steam-cycle tomogram indicates that the Poisson's ratio has decreased by approximately 0.10 in reservoir zones near the cyclic and continuous injectors, as shown in Figure 21.

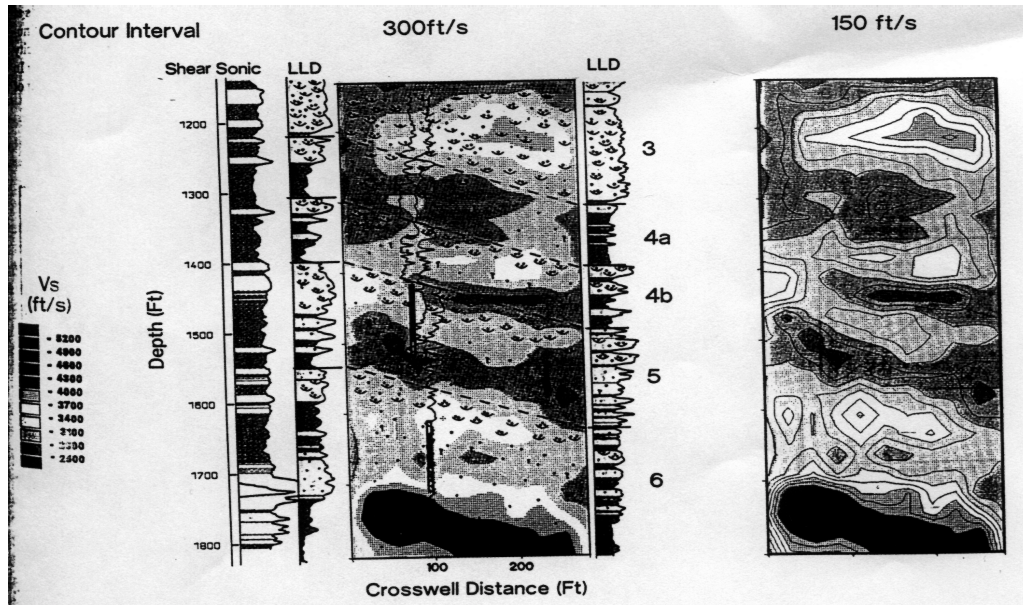


FIG. 20. Baseline S-wave tomogram which images crosswell structure, lithofacies and porosity variations. Sand facies variations are documented by resistivity (LLD) logs. Channel sands with excellent reservoir quality are imaged by higher velocities than moderate reservoir quality bioturbated levee sands. Heterogeneity within each 300 ft/s velocity field is indicated by the corresponding plot with 150 ft/s contour intervals (Mathisen et al., 1995).

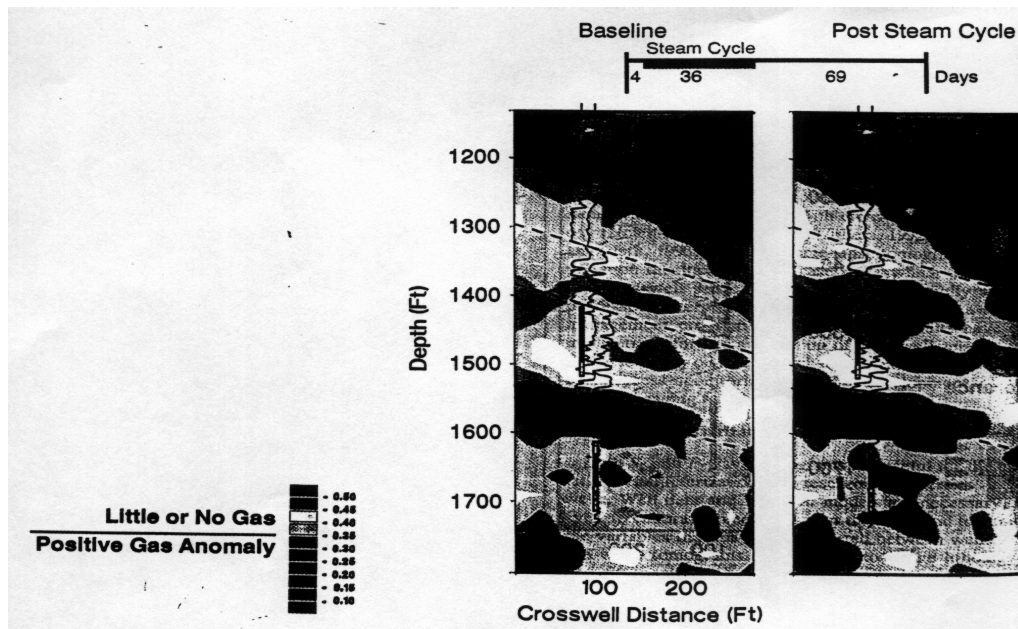


FIG. 21. Baseline and post-steam cycle Poisson's ratio tomograms documenting increase in gas near injectors after steam cycle. Baseline tomogram positive gas anomalies are a result of previous cyclic steaming (Mathisen et al., 1995).

## Time-lapse seismic surveys in Pikes Peak, Saskatchewan

The Pikes Peak thermal project was initiated in 1981 to mobilize heavy oil with a density of 0.99 (g/cm<sup>3</sup>) and a viscosity of 25,000 cp at a reservoir temperature of 18°C (Miller and Steiger, 1999). Production is from the Waseca sands of the lower Cretaceous buried at 500 m and having a porosity of 32-36% and a permeability of 4500-10,000 mD (Miller and Steiger, 1999). Recovery efficiency to September 1995 had reached 52% (Miller and Steiger, 1999). Seismic monitoring of steam fronts may lead to further recovery. Watson and Lines (2000) inverted the acoustic impedance of the reservoir from a 2-D seismic swath line and found that a low acoustic impedance zone corresponds to the area where steam was injected. Downton and Lines (2001) processed the vertical component of the 3-C seismic line in an amplitude preserving fashion. Figure 22 shows a strong amplitude at 0.49 seconds, which is at the base of the channel. This is due to four injection wells close to the seismic line. Additional results are found in this volume (Watson and Lines, 2001).

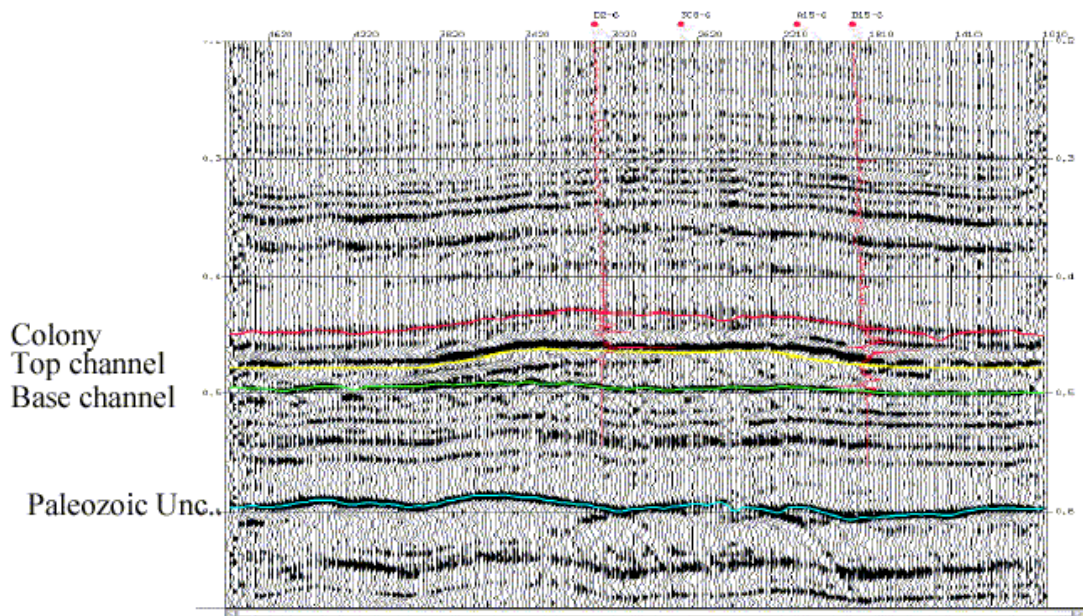


FIG. 22. Strong amplitude at the base of the channel (Downton and Lines, 2000)

## CONCLUSIONS

Heavy oil reservoirs contain huge reserves of hydrocarbons and will be an important source of energy for Canada and the world. Thermal methods are the major EOR processes for heavy oil reservoirs. Steamfloods lead to a steam zone near the injection location, a hot water zone, a hot water and oil zone, a hot oil zone and the cold reservoir zone. Due to the natural heterogeneity of the geological materials, steam fronts tend to propagate irregularly along zones of high permeability.

Knowledge of steam front distributions and the geometry of the surrounding fluid zones allows reservoir engineers to make more efficient production decisions.

The sands and rocks that contain heavy oil reserves tend to be weak with low bulk and shear moduli and, consequently, fluid substitution effects cause large changes in the moduli. The bulk modulus and density of steam are much different than that of heavy oil and water, making steam fronts good targets for seismic monitoring. Many examples of successful steam monitoring have been presented. Seismic changes that have most commonly been used to monitor steam fronts are changes in the time between events above and below the producing horizon, velocity changes and reflection amplitude changes. However, the complex interactions lead to complex seismic response changes. Recent work has shown that using an array of seismic attributes along with statistical techniques such as discriminant analysis can lead to high resolution mapping of steam fronts and chambers. Future work remains to determine the best ways to calibrate images and to better map the fluid zones away from the steam front.

## REFERENCES

- Agar, A.G., Morgenstern, N.R., and Scott, J.D., 1986, Thermal expansion and pore pressure generation in oil sands, *Can. Geotech. Journal*, 23, 327-333.
- Agar, A.G., Morgenstern, N.R., and Scott, J.D., 1987, Shear strength and stress-strain behavior of Athabasca oil sand at elevated temperature and pressure, *Can. Geotech. Journal*, 24, 1-10.
- Bregman, N.D., Hurley, P.A., and West, G.F., 1989, Seismic tomography at a fire-flood site, *Geophysics*, 54, 1082-1090.
- Britton, M.W., Martin, W.L., Leibrecht, R.J., and R. A. Harmon, 1983, Street Ranch pilot test of fracture-assisted steamflood, *JPT*, 35, 511-522.
- den Boer, L.D. and Matthews, L.W., 1988, Seismic characterization of thermal flood behaviour, 4<sup>th</sup> UNITAR/UNDP conference on heavy oil crude and tar sands, paper no. 94.
- Downton, J.E. and Lines, L.R., 2000, Preliminary results of the AVO analysis at Pikes Peaks, the CREWES report, 12, 523-531.
- Eastwood, J., 1994, Seismic monitoring of steam-based recovery of bitumen, *The Leading Edge*, 13, 242-251.
- Gendzwill, D.J., 1992, Passive seismic monitoring of hydrofracture and steam injection in heavy oil sands near Fort McMurray, Alberta, *Canadian Journal of Exploration Geophysics*, 28(2), 117-127.
- Greaves, R.J. and Fulp, T.J., 1987, Three-dimensional seismic monitoring of an enhanced oil recovery process, *Geophysics*, 52, 1175-1187.
- Isaac, J.H., 1996, Seismic methods for heavy oil reservoir monitoring, Ph.D. thesis, University of Calgary.
- Jenkins, S.D., Waite, M.W., and Bee, M.F., 1997, Time-lapse monitoring of the Duri steamflood: A pilot and case study, *The Leading Edge*, 16(9), 1267-1273.
- Jack, I., 1998, Time-lapse seismic in reservoir management, SEG course notes.
- Kalantzis, F., 1994, Imaging of reflection seismic and radar wavefields: Monitoring of steam-heated oil reservoirs and characterization of nuclear waste repositories, Ph.D. thesis, University of Alberta.
- Laine, E.F., 1987, Remote monitoring of the steam-flood enhanced recovery process, *Geophysics*, 52, 1457-1465.
- Lake, L.W., 1989, *Enhanced oil recovery*, New Jersey: Prentice-Hall, Inc.
- Lumley, D.E., 1995, 4-D seismic monitoring of an active steamflood, the 65<sup>th</sup> SEG annual meeting, Expanded Abstracts, 203-206.

- Macrides, C.G., Kanasewich, E.R. and Baratha, S., 1988, Multiborehole seismic imaging in steam injection heavy oil recovery projects, *Geophysics*, 53, 65-75.
- Mathisen, M.E., Vasiliou, A.A., Cunningham, P., Shaw, J., Justice, J.H., and Guinzy, N.J. 1995, Time-lapse crosswell seismic tomogram interpretation: Implications for heavy oil reservoir characterization, thermal recovery process monitoring, and tomographic imaging technology, *Geophysics*, 60(3), 631-650.
- Mathisen, M.E., Cunningham, P., Shaw, J., Vasiliou, A.A., Justice, J.H., and Guinzy, N.J., 1995, Crosswell seismic radial survey tomograms and the 3-D interpretation of a heavy oil steamflood, *Geophysics*, 60(3), 651-659.
- Miller, K.A. and Steiger, R.A. 1999, Pikes Peak project: Successful without horizontal wells, *JCPT*, 38(4), 21-26.
- Nur, A., 1989, Four-dimensional seismology and (true) direct detection of hydrocarbons: The petrophysical basis, *The Leading Edge*, 8(2), 30-36.
- Paulsson, B.N.P., Meredith, J.A., Wang, Z., and Fairborn, J.W. 1994, The Steepbank crosswell seismic project: reservoir definition and evaluation of steamflood technology in Alberta tar sands, *The Leading Edge*, 13(6), 737-747.
- Paulsson, B.N.P., Smith, N.E., Tucker, K.A., and Fairborn, J.W. 1992, Characterization of a steamed oil reservoir using cross-well seismology, *The Leading Edge*, 11(6), 24-32.
- Pullen, N., Matthews, L., and Hirsche, K., 1987, Techniques applied to obtain very high resolution 3-D seismic imaging at an Athabasca tar sands thermal project, *The Leading Edge*, 6 (12), 10-15.
- Snell, J.S. and Close, A.D. 1999, Yates field steam pilot applies latest seismic and logging monitoring techniques, *SPE* 56791.
- Sun, S. (Z.), 2001, Reservoir monitoring and characterization for heavy oil thermal recovery, *Recorder*, 26(8), 28-36.
- Thakur, G., 1998, Heavy oil reservoir management, *The 15<sup>th</sup> World Oil Petroleum Congress*, Abstracts, 422-426.
- Tosaya, C.A. and Nur, A.M., 1984, Monitoring of thermal EOR fronts by seismic methods, *SPE* 12744
- Waite, M. W., Rusdinadar S., Rusdibiyo, A.V., Susanto, T. Primadi H., and Satrina, D., 1997, Application of seismic monitoring to manage an early-stage steamflood, *SPE Reservoir Engineering*, 277-283.
- Walters, D.A., Settari, A., and Kry, P.R., 2000, Poroelastic effects of cyclic steam stimulation in the Cold Lake reservoir, *SPE* 62590, 1-10.
- Wang, Z. and Nur, A., 1988, Seismic velocities in heavy oil and tar sands: The basis for in-situ recovery monitoring, 4<sup>th</sup> UNITAR/UNDP conference on heavy oil crude and tar sands, paper no. 110.
- Watson, I. and Lines, L.R., 2001, Heavy oil time-lapse seismic monitoring at Pikes Peak, Saskatchewan, the CREWES Report, 13,wa2(1-7).
- Watson, I. and Lines, L.R., 2001, Time-lapse seismic monitoring at Pikes Peak, Saskatchewan, CSEG national convention, Extended Abstracts, 6-8.
- Watson, I., Brittle, K.F. and Lines, L.R., 2001, Heavy-oil reservoir characterization using elastic wave properties, the CREWES Report, v. 13.
- Wilt, M., Schenkel, C. Daley, T. Peterson, J. Majer, E., Murer, A.S., Johnston, R.M., and Klonsky, L., 1995, Mapping steam and water flow in petroleum reservoirs, *SPE reservoir engineering*, 284-287
- Zhang, J.J., 2001, Time-lapse seismic surveys: Rock physics, M. Sc. Thesis, University of Calgary.